

泥页岩中有机质-黏土复合体的微观结构、变形作用及源-储意义

李晓霞¹, 谷渊涛^{1,2}, 万泉³, 杨曙光³

(1. 河南工程学院 环境与生物工程学院, 河南 郑州 451191; 2. 南京大学 地理与海洋科学学院, 江苏 南京 210023; 3. 中国科学院 地球化学研究所 矿床地球化学国家重点实验室, 贵州 贵阳 550081)

摘要:泥页岩中的有机质和黏土矿物在沉积演化过程中能够相互结合形成有机质-黏土复合体, 成为重要的生烃母质。基于大量的场发射扫描电镜和透射电镜观察分析, 以中国鄂尔多斯盆地三叠系延长组、黔北奥陶系-志留系五峰组-龙马溪组、黔中寒武系牛蹄塘组及南华北盆地二叠系山西组4套泥页岩储层为研究对象, 详细查明了泥页岩中有机质-黏土复合体的微观结构及变形作用, 并深入探讨了其源-储意义。泥页岩中有机质-黏土复合体成分复杂, 形态多样, 且易发生变形; 驱动复合体发生变形的机制有构造应力作用、矿物颗粒作用、有机质赋存及黏土矿物转化。其中, 由外部构造应力和复合体内部矿物颗粒对黏土层、有机质层挤压引起的变形能够改变复合体局部应力环境, 所形成的拉张环境可使复合体发育大量纳米孔隙, 且这些孔隙因黏土层的保护而不易发生烃类散失, 可有效提升泥页岩的储集能力。相关结论有助于完善泥页岩的成岩理论, 增进对页岩油气生成、运移和储集过程的认识, 进而指导页岩油气的勘探开发。

关键词:微观结构; 变形作用; 拉张环境; 储集能力; 有机质-黏土复合体; 泥页岩

中图分类号: TE122.1 **文献标识码:** A

Micro-architecture, deformation and source-reservoir significance of organic-clay composites in shale

LI Xiaoxia¹, GU Yuantao^{1,2}, WAN Quan³, YANG Shuguang³

(1. School of Resources and Environment, Henan University of Engineering, Zhengzhou, Henan 451191, China; 2. School of Geography and Ocean Science, Nanjing University, Nanjing, Jiangsu 210023, China; 3. State Key Laboratory of Deposit Geochemistry, Institute of Geochemistry, Chinese Academy of Sciences, Guiyang, Guizhou 550081, China)

Abstract: The organic matter and clay minerals in shale can combine with each other to form organic-clay composites during sedimentation and evolution, which are an important source of parent materials of hydrocarbons. An integration of field emission scanning electron microscopy (FE-SEM) and transmission electron microscopy (TEM) is applied to study the deformation and micro-architecture of organic-clay composites, and discuss their source-reservoir significance in depth. The object of study is the four suites of typical shale reservoirs, that is, the Triassic Yanchang Formation of the Ordos Basin, the Ordovician Wufeng-Silurian Longmaxi formations of northern Guizhou, the Cambrian Niutitang Formation of central Guizhou, as well as the Permian Shanxi Formation of the Southern North China Basin. The organic-clay composites in shale feature complex components, diverse geometries and being prone to deform, and the main mechanisms driving the deformation mainly include tectonic stress, mineral particles, the occurrence of organic matter and the transformation of clay minerals. The deformation caused by tectonic stress outside the composites and mineral particles (imposed on the surrounding clay layer and organic layer) inside the composites could change the local stress environment of the composites, resulting in extensional environment, which could in turn drive the large-scale development of nano-pores in the composites. Under the protection of clay layer, hydrocarbons stored in the nano-pores

收稿日期:2022-08-02; 修订日期:2022-12-20。

第一作者简介:李晓霞(1988—),女,博士,讲师,细粒沉积学。E-mail: lixiaox88@163.com。

基金项目:国家自然科学基金项目(41802143);河南省自然科学基金项目(212300410129);矿床地球化学国家重点实验室开放基金项目(201904);河南工程学院博士基金项目(DKJ 2018014, DKJ 2018015)。

are less likely to loss, which could effectively improve the storage capacity of shale reservoir. The conclusions achieved in the study are of beneficial value to understanding the diagenetic evolution of shale, as well as the generation, migration and storage of shale oil and gas, thus guiding the exploration and development of shale oil and gas.

Key words: micro-architecture, deformation, extensional environment, storage capacity, organic-clay composite, shale

引用格式: 李晓霞, 谷渊涛, 万泉, 等. 泥页岩中有机质-黏土复合体的微观结构、变形作用及源-储意义[J]. 石油与天然气地质, 2023, 44(2): 452-467. DOI: 10. 11743/ogg20230216.

LI Xiaoxia, GU Yuantao, WAN Quan, et al. Micro-architecture, deformation and source-reservoir significance of organic-clay composites in shale [J]. Oil & Gas Geology, 2023, 44(2): 452-467. DOI: 10. 11743/ogg20230216.

泥页岩和海洋沉积物中的有机质-黏土相互作用是有机质保存和全球碳循环的重要机制^[1-3]。与脆性矿物(如石英、长石等)不同,泥页岩中的有机质和黏土矿物具有物理、化学活性,可通过静电作用、离子偶极力、氢键和范德华力等方式相互结合^[4-8]。这种结合体被国内外学者称之为有机质-黏土复合体^[2-3, 9-13]。泥页岩中的有机质-黏土复合体已被证实是重要的生烃母质,并参与了有机质的聚集、沉积、保存及成岩过程,且对有机质抵抗生物降解、氧化、水解等过程有重要的保护作用,从而使有机质得以大量保存^[14-17]。泥页岩在埋藏过程中经历了复杂的成岩演化过程,严重影响着储层发育特征^[18-22]。有机质-黏土复合体具有明显不同于黏土矿物和有机质的独特结构和性质^[2, 11],对于成岩演化的响应也具有特殊性和复杂性。首先,有机质在成岩演化过程中受应力作用可发生变形,并影响有机质孔隙形态^[23];黏土矿物在深埋藏条件下可发生矿物转化,改变黏土结构与性质^[15, 24-25]。本研究在前期发现,泥页岩中的有机质-黏土复合体在成岩演化过程中也存在明显的变形作用^[26],但其变形机制与响应尚不清楚。其次,在黏土矿物催化作用下,有机质-黏土复合体的生烃作用十分显著^[17, 27],是泥页岩中烃类生成的重要来源,但目前尚无关于有机质-黏土复合体的储集作用研究。

本研究通过采集4套典型泥页岩(鄂尔多斯盆地三叠系延长组、黔北奥陶系-志留系五峰组-龙马溪组、黔中寒武系牛蹄塘组及南华北盆地二叠系山西组)样品,利用场发射扫描电镜(FE-SEM)和透射电镜(TEM)精细表征了有机质-黏土复合体的微观结构,分析了有机质-黏土复合体的变形作用和机制,并就其源-储意义进行了深入探讨。相关结论可为提升研究区页岩油气的勘探开发成效提供借鉴。

1 地质背景

华北板块西部的鄂尔多斯盆地具有克拉通内盆地属性和特征,是中国最稳定的构造单元之一^[28],主要

由6个构造单元组成(图1a)。页岩油气资源主要分布于伊陕斜坡^[29-30]。鄂尔多斯盆地延长组主要发育淡水陆相盆地,盆内湖相碎屑岩可进一步划分为10段,其中的延长组7段(长7段)沉积期水体深度大,形成了一套富含有机质的泥页岩夹砂岩,是页岩油气勘探开发的重点目标层位^[30-34]。本研究所采用的延长组样品均源于长7段泥页岩,采自伊陕斜坡东南部(图1a)。该区域延长组主要形成于滨浅湖沉积相,长7段厚度相对较小(<30 m)^[31]。

本研究选取的五峰组-龙马溪组和牛蹄塘组位于四川盆地东南缘,区域内志留系-寒武系广泛发育富含有机质泥页岩,是页岩气勘探开发的主要目标层位^[35-36]。五峰组-龙马溪组剖面处于四川盆地东南部的黔北地区(图1b),该区域龙马溪组下部硅质页岩发育,富含有机质,主要形成于贫氧/缺氧环境^[37-38]。此后,海平面下降和底流沉积作用破坏了缺氧环境,同时由于沉积速率较快,在龙马溪组上部形成了黏土质、粉砂质页岩^[37-43],且有机质含量相对较低。牛蹄塘组位于黔中隆起东部(图1b),其下部形成于深水陆棚沉积环境,发育一套炭质泥页岩;上部主要形成于浅水陆棚环境,岩性以钙质泥质粉砂岩、粉砂质泥页岩为主^[44-46]。该区域牛蹄塘组由于构造作用强烈遭受抬升、剥蚀,断裂十分发育,地层以低压-常压为主,保存条件较差,页岩气散失较为严重^[47]。

南华北盆地上古生界发育有广泛的煤层和泥页岩储层,该区域(图1c)的页岩气调查表明山西组海-陆过渡相泥页岩是潜在的烃源岩^[48],其沉积特征、岩性组合、分布特征等与上述陆相、海相地层有明显差异。首先,山西组沉积环境由前三角洲逐渐向三角洲前缘演化,最终演化为三角洲平原沉积,总体呈现为海退进积序列^[48-49]。其次,山西组下部发育砂岩层段,上部以黑色泥岩与煤层为主,形成一套三角洲沉积体系的泥页岩和细-粉砂岩,夹煤层(二1煤层)^[49-50]。另外,山西组富含有机质泥页岩单层厚度小,常与砂岩、粉砂岩互层,累计厚度较大,且横向分布特征有较大变化^[48]。

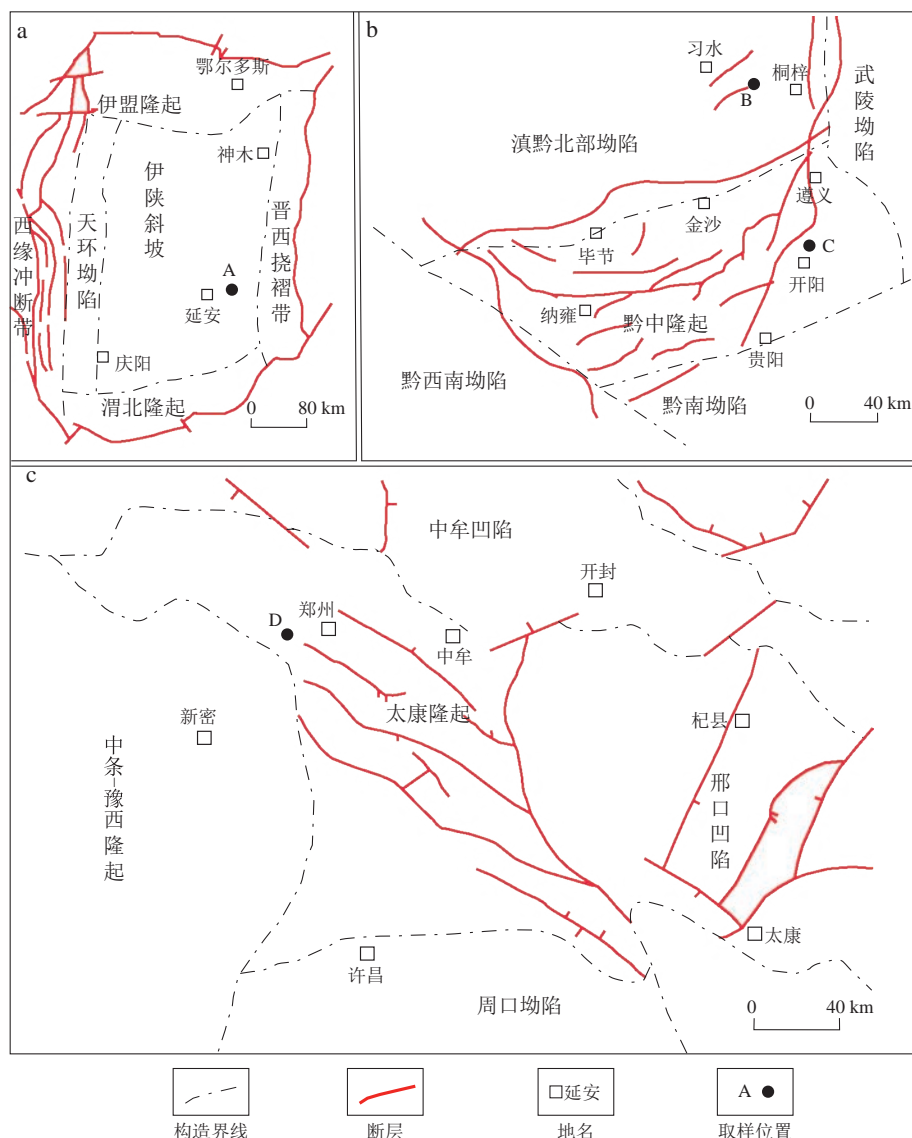


图1 鄂尔多斯盆地延长组、黔北五峰组-龙马溪组、黔中牛蹄塘组及南华北盆地山西组泥页岩取样位置及地质概况^[29,51]

Fig. 1 Maps showing the sampling locations and regional geology of the Yanchang Formation in the Ordos Basin, Wufeng-Longmaxi formations in northern Guizhou, Niutitang Formation of central Guizhou, and Shanxi Formation in the Southern North China Basin^[29,51]

a. 鄂尔多斯盆地; b. 黔北及黔中地区; c. 南华北盆地太康隆起

A. 941#采油井; B. 骑龙村剖面; C. ZK105钻孔; D. ZK02109钻孔

2 泥页岩组成特征

本研究分析了4套地层的泥页岩样品共58件,取样位置见图1。其中,延长组(15件)、牛蹄塘组(14件)和山西组(14件)样品均为钻孔样品,分别取自941#采油井,ZK105钻孔和ZK02109钻孔。五峰组-龙马溪组(15件)样品取自贵州习水县骑龙村露头剖面,采用绍尔便携式取样钻机获取浅层钻孔样品,降低了表层风化作用对储层特征分析的影响。

图2显示了各组样品具体的取样深度、岩性及组

成特征。长7段泥页岩(图2a)总有机碳含量(TOC)垂向上分布较为均匀(其中12个样品的 TOC 分布在2.0%~3.9%);镜质体反射率(R_o)为0.7%~1.4%,平均为1.0%,说明长7段沉积环境较为稳定,形成了中-低成熟度的富有机质泥页岩。五峰组-龙马溪组泥页岩(图2b) TOC 分布在0.3%~5.5%,平均2.6%; R_o 分布在2.5%~3.1%,平均2.8%。骑龙村剖面第一段页岩 TOC 从底至顶呈明显降低的趋势,证实了沉积环境由深水陆棚相向浅水陆棚相的过渡^[38]。与龙马溪组类似,从底至顶牛蹄塘组泥页岩(图2c)样品的 TOC 也呈降低趋势,其范围为0.3%~5.5%,平均2.2%;这与

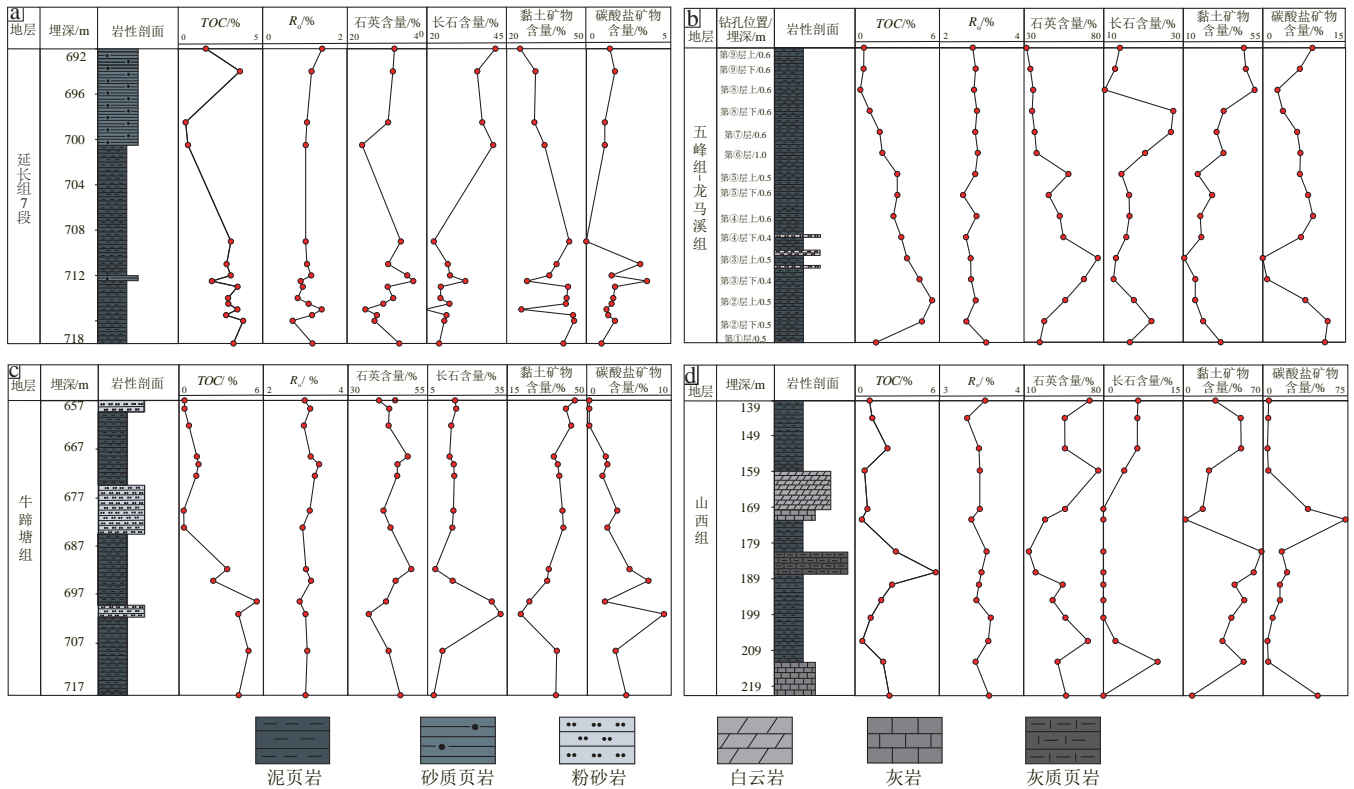


图 2 鄂尔多斯盆地延长组、黔北五峰组-龙马溪组、黔中牛蹄塘组及南华北盆地山西组泥页岩储层的组成特征

Fig. 2 Composition characteristics of the shale samples from the Yanchang Formation in the Ordos Basin, Wufeng-Longmaxi formations in northern Guizhou, Niutitang Formation of central Guizhou, and Shanxi Formation in the Southern North China Basin
a. 长 7 段, 941# 采油井; b. 五峰组-龙马溪组, 样品取自浅钻; c. 牛蹄塘组, ZK105 钻孔; d. 山西组, ZK02109 钻孔

该区域另一钻孔(ZK403)的 TOC 变化趋势较为一致, 以上结果均表明研究区内牛蹄塘组沉积环境由深水陆棚相逐渐向浅水陆棚相过渡^[52]。牛蹄塘组泥页岩的 R_o 范围在 2.8% ~ 3.3%, 平均 3.1%, 处于高-过成熟阶段。山西组(图 2d)样品的 TOC 在 0.5% ~ 5.8%, 平均 1.9%, 在垂向上的分布较不均匀, 无明显变化规律, 这是由海-陆过渡相沉积环境导致的水深快速变化所引起的。山西组样品 R_o 范围为 3.3% ~ 3.6%, 平均 3.5%, 处于过成熟阶段; 该地层沉积期晚于牛蹄塘组和龙马溪组, 但后期的区域热事件导致该地层具有更高的热成熟度^[46, 53]。

图 2 中的矿物成分表明延长组、五峰组-龙马溪组和牛蹄塘组样品主要由石英、黏土矿物和长石组成, 碳酸盐矿物含量均较低。总体上, 五峰组-龙马溪组和牛蹄塘组样品的石英含量(平均值分别为 47% 和 44%) 明显高于延长组(平均值为 30%), 长石含量(平均值分别为 17% 和 15%) 则相对较低(延长组的平均值为 29%); 五峰组-龙马溪组样品具有比牛蹄塘组和延长组更低的黏土矿物含量(前者平均值为 28%, 后两者的分别为 35% 和 37%), 更高的碳酸盐矿物含量(前者的

组平均值为 7%, 后两者的分别为 3% 和 2%)。这 3 套样品的矿物成分表明五峰组-龙马溪组和牛蹄塘组泥页岩脆性矿物含量高, 可压裂性强。山西组样品的矿物组成变化明显, 这是由于海-陆过渡相沉积环境快速变化导致陆源碎屑沉积物质(如石英和长石)和内源沉积物质(如碳酸盐矿物)呈现出此消彼长的关系。

3 有机质-黏土复合体微观结构

利用氩离子抛光-扫描电镜对 4 套泥页岩样品观察, 发现有有机质-黏土复合体分布广泛并呈现多种形态特征(图 3)。根据复合体中黏土矿物片层之间的接触方式, 可将复合体分为条带状和卡房状(图 4)。黏土沉积时, 介质中富 Na^+ 和酸性环境可使黏土的边缘带正电, 从而有利于边(+)/面(-)接触的形成(图 4a), 碱性沉积环境且介质中富 Ca^{2+} 有利于黏土层形成面(-)/面(-)接触(图 4b)^[54-55]。条带状复合体即黏土层以面(-)/面(-)接触的方式与有机质在后期演化过程中相结合所形成, 往往呈现出有机质和黏土矿物成层分布特征(图 3b-d, f-h, j)。而卡房状复合体则是黏土

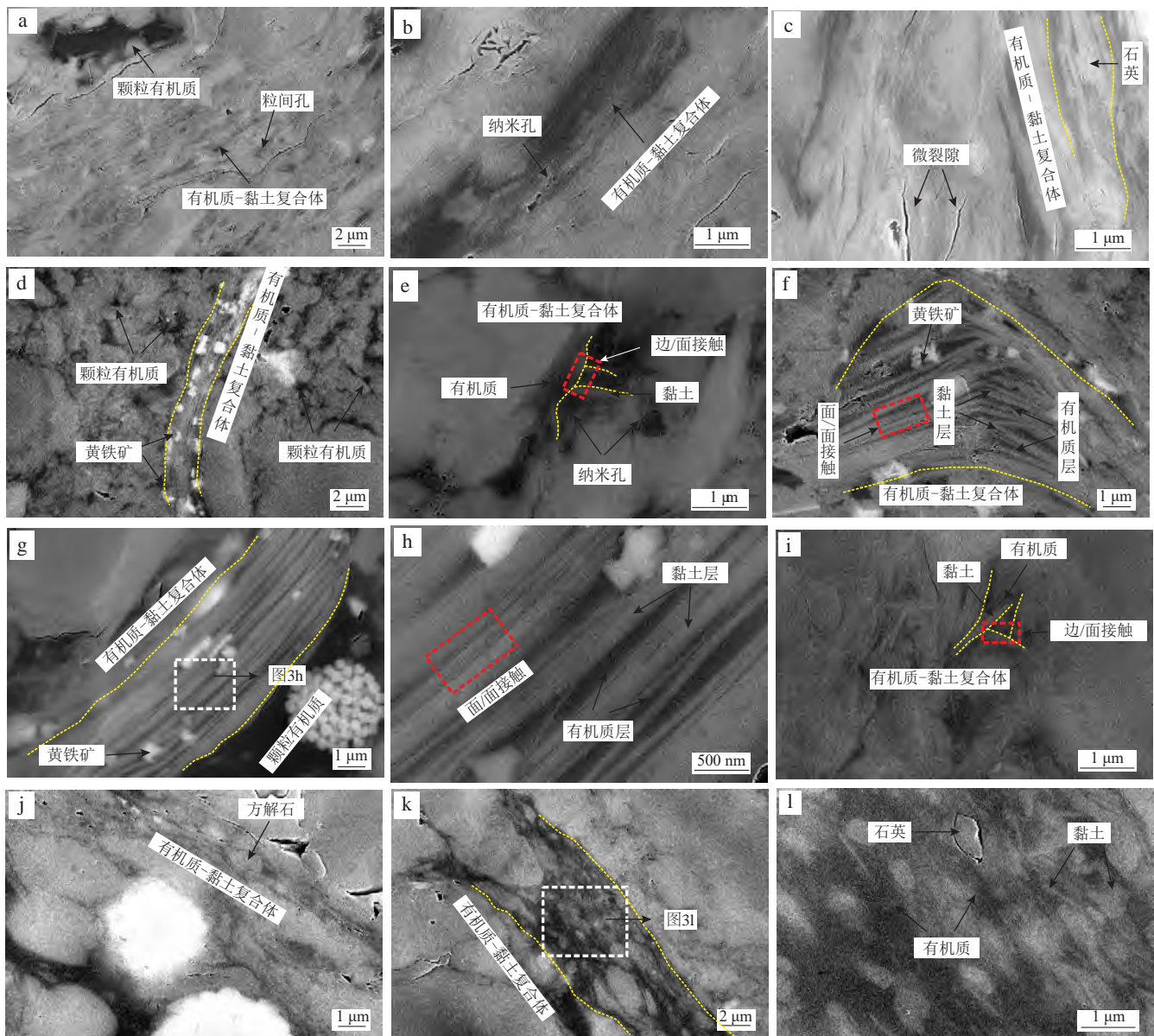


图3 鄂尔多斯盆地延长组、黔北龙马溪组、黔中牛蹄塘组及南华北盆地山西组泥页岩中有机质-黏土复合体的SEM图像
Fig. 3 SEM images of organic-clay composites in the shale samples from the Yanchang Formation in the Ordos Basin, Wufeng-Longmaxi formations in northern Guizhou, Niutitang Formation of central Guizhou, and Shanxi Formation in the Southern North China Basin
a—c. 长7段, 941#采油井, 埋深716.0 m; d—f. 龙一段第②层浅钻, 埋深0.5 m; g—i. 牛蹄塘组, ZK105钻孔, g和h图埋深为701.0 m, i图埋深为670.0 m; j—l. 山西组, ZK02109钻孔, 埋深222.7 m

[b—d, f—h和j图显示了条带状复合体的分布特征; e图和i图显示了卡房状复合体的分布特征; a, k和l图中的复合体则明显有其他矿物(如石英、方解石)的介入, 导致复合体形态较为复杂。红色虚线框指示黏土的接触方式; 黄色虚线指示黏土的延伸方向。]

层以边(+)/面(-)接触方式沉积后, 在黏土被显著压实之前发生了被动充填(可能是生物化石)^[56-57], 从而使该结构能够保存下来(图3e, i)。

根据有机质-黏土复合体是否发生变形, 可将其分为原始复合体和变形复合体。由于复合体经历了成岩演化过程, 受多种应力作用, 大多数复合体可能发生一定程度的变形(图3c, d, f, g), 从而表现为三角形

状(图3f)、透镜体状(图3g)及不规则状(图3c, k)。具有卡房结构的黏土在后期被充填后具有一定的结构稳定性, 可能保持了原始形态(图3e, i没有发生明显变形)。此外, 部分复合体既无明显的卡房结构, 也没有明显的条带状分布特征, 有机质和黏土之间界线模糊, 分布混乱(图3l)。这是因为复合体在沉积和成岩过程中被其他因素如脆性矿物颗粒嵌入、黏土矿物转化等

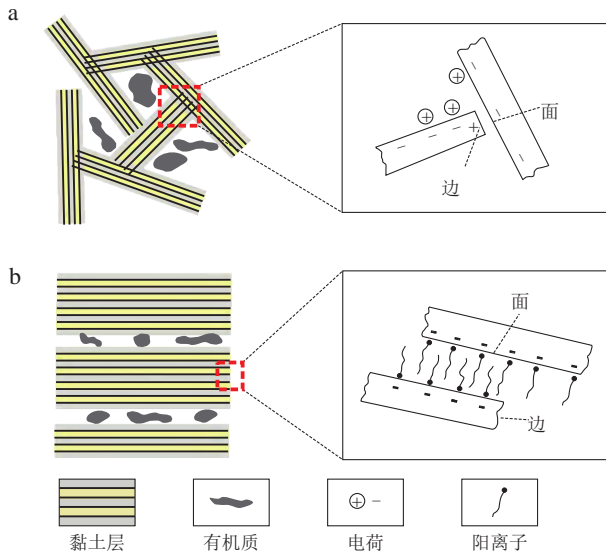


图4 黏土层卡房结构和条带结构示意图^[54]

Fig. 4 Sketch diagrams showing the card-house and band-like architectures of the clay layers^[54]

a. 卡房结构及边(+)/面(-)接触; b. 条带结构及面(-)/面(-)接触

所干扰,从而形成了极为复杂的形态特征。

为了深入探讨有机质-黏土复合体的变形机制和影响因素,利用聚焦离子束-扫描电镜(FIB-SEM)进行典型复合体的TEM制样,以分析引起复合体变形的主要因素。如图5所示,分别选取了4套样品中发生变形的典型复合体进行FIB切割,制成长宽均为10 μm,厚度小于80 nm的薄片进行TEM观察。TEM明场(bright field)图像表明不同样品的复合体结构和成分特征均有明显差异(图6):龙马溪组(图6c)和牛蹄塘组样品的复合体(图6e, f)中发育大量黄铁矿,而延长组(图6a, b)和山西组样品的复合体(图6g, h)中则基本没有黄铁矿,上述代表性视域与SEM观察结果一致(图3)。推测是由于研究区延长组为滨浅湖沉积环境,山西组为三角洲沉积环境,这两种沉积环境均不利于黄铁矿的形成和保存;相比之下,五峰组-龙马溪组和牛蹄塘组为深水陆棚相沉积,形成于偏还原的水体环境,更有利于黄铁矿的形成。此外,龙马溪组和牛蹄塘组样品中的复合体呈现出有机质和黏土矿物成层分布特征(图6c-f);而延长组和山西组样品中复合体的有机质和黏土矿物分布较为混乱(图6a, b, g, h),无明显规律。针对上述差异,对延长组和山西组泥页岩中的复合体进行局部放大,发现黏土层存在较多的边(+)/面(-)接触(图6b, h),且形态极不规则。考虑到延长组和山西组的沉积环境,陆源碎屑矿物引入较多,因而打乱了黏土层沉积时的规律分布,使得其形态不同于龙马溪组、牛蹄塘组样品中成层分布的复合体。

4 有机质-黏土复合体变形机制

有机质-黏土复合体的变形是泥页岩成岩演化的重要组成部分,其变形机制十分复杂。通过大量的FE-SEM和TEM观察分析,认为引起泥页岩中有机质-黏土复合体发生变形的因素主要有以下4个方面。

4.1 构造应力作用

研究区龙马溪组和牛蹄塘组均处于构造改造作用较强烈地区,应力环境复杂,应力作用与有机质-黏土复合体变形密切相关。如图7所示,有机质-黏土复合体周围均发育明显的微裂隙,且复合体具有显著的变形特征。例如,图7a和7b中的复合体为三角形,图7c中的复合体发生了一定程度的错位,造成黏土层延伸方向不一致,图7d则形成了透镜体状的复合体。复合体的上述变形特征表明其处于一定的应力环境中,部分复合体的变形特征可用于判断相应区域的应力方向。图7c中右侧复合体的黏土层(红色虚线)与左侧的延伸方向(黄色虚线)不一致,表明其受到剪切力的作用(应力方向为红色箭头所指方向)。图7d中在复合体边缘的长石由于剪切作用发生断裂,左侧长石相对向下移动,右侧长石相对向上移动,同时,由于有机质和黏土矿物均有较强的塑性变形能力,使得复合体不易断裂而发生透镜体状的变形。

4.2 矿物颗粒作用

SEM和TEM观察结果显示有机质-黏土复合体中除黏土矿物外,还存在大量的矿物颗粒(图3,图6),受矿物颗粒支撑影响,复合体结构发生一定变化。延长组(图6a)和山西组泥页岩(图6g, h)中的复合体在视域范围内存在较多的脆性矿物颗粒,对复合体的微观结构有明显的扰动作用。如图8所示,延长组泥页岩复合体中发育石英、方解石、长石、铁氧化物等矿物颗粒,这些矿物引起周围的黏土层发生明显的变形作用。龙马溪组(图6c)和牛蹄塘组(图6e, f)复合体中没有观察到脆性矿物颗粒,但赋存有大量的黄铁矿颗粒,这些颗粒往往发育在有机质层,被两个黏土层所夹持,意味着黄铁矿和有机质可能是同时沉积并被保存了下来,这对于有机质的赋存和生烃有重要意义。

4.3 有机质的赋存

根据有机质的稳定性,前人将泥页岩中的有机碳分为稳定有机碳和活性有机碳^[58]。其中,活性有机碳

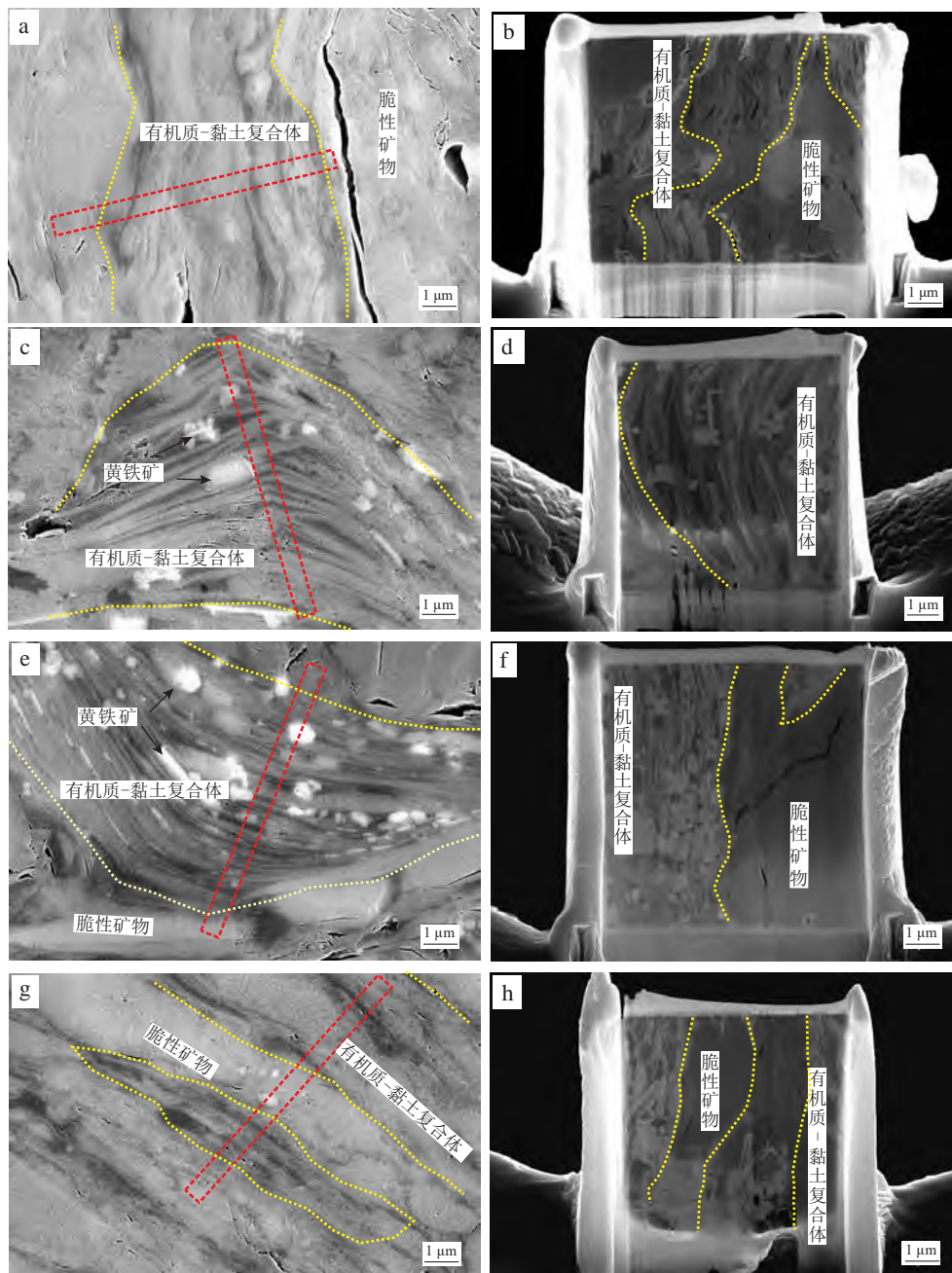


图5 鄂尔多斯盆地延长组、黔北龙马溪组、黔中牛蹄塘组及南华北盆地山西组泥页岩中选取的进行FIB切片的典型有机质-黏土复合体SEM图像

Fig. 5 SEM images showing typical organic-clay composites selected for focus ion beam (FIB) slicing from the shale samples of the Yanchang Formation in the Ordos Basin, Wufeng-Longmaxi formations in northern Guizhou, Niutitang Formation of central Guizhou, and Shanxi Formation in the Southern North China Basin

a, b. 长7段, 941#采油井, 埋深716.0 m; c, d. 龙一段第②层浅钻, 埋深0.5 m; e, f. 牛蹄塘组, ZK105 钻孔, 埋深701.0 m; g, h. 山西组, ZK02109 钻孔, 埋深222.7 m

(a, c, e 和 g 中, 黄色虚线指示所选取复合体的平面展布, 红色虚线框指示了切片方向和位置; b, d, f 和 h 右侧为利用 FIB 制成的薄片, 厚度 <80 nm, 其中黄色虚线指示了复合体的纵向延伸方向。)

主要赋存于孔隙或黏土矿物层间的边缘(物理活性有机碳)部位或吸附在黏土矿物的外表面(化学活性有机碳), 而稳定有机碳主要赋存于黏土矿物的内表面^[58]。本研究通过 FE-SEM 和 TEM 分析发现有机质-黏土复

合体中的有机质主要赋存位置有两种: 多层层间和单层层间, 均处于黏土矿物层间, 推测这两类有机质为稳定有机碳。多层层间有机碳主要分布在卡房状复合体所形成的“房”中, 或以条带状分布于数十纳米厚的黏

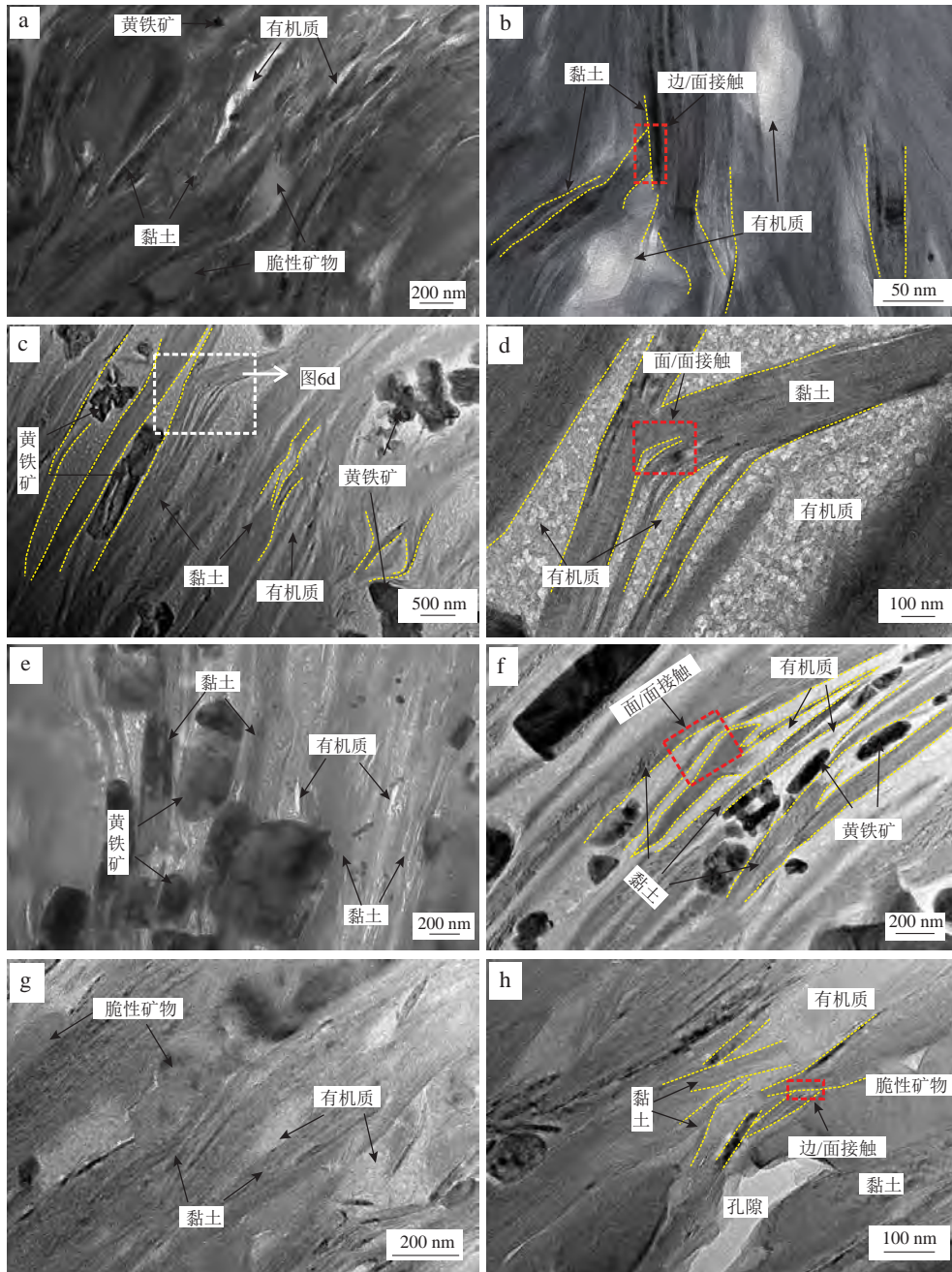


图6 鄂尔多斯盆地延长组、黔北龙马溪组、黔中牛蹄塘组及南华北盆地山西组泥页岩中有机质-黏土复合体的TEM图像
 Fig. 6 Transmission electron microscopy (TEM) images of organic-clay composites in the shale samples from the Yanchang Formation in the Ordos Basin, Wufeng-Longmaxi formations in northern Guizhou, Niutitang Formation of central Guizhou, and Shanxi Formation in the Southern North China Basin
 a, b. 长7段, 941#采油井, 埋深716.0 m; c, d. 龙一段第②层浅钻, 埋深0.5 m; e, f. 牛蹄塘组, ZK105 钻孔, 埋深701.0 m; g, h. 山西组, ZK02109 钻孔, 埋深222.7 m
 (红色虚线框指示黏土层的接触方式; 黄色虚线指示黏土层的延伸方向。)

土矿物层间(图9中的“碳”元素分布), 单层层间有机碳则主要分布在可膨胀黏土矿物(如蒙脱石或伊/蒙混层)1~2 nm厚的层间。

这两种赋存方式均可造成有机质-黏土复合体的变形。多层层间有机碳常与黄铁矿颗粒伴生, 从而引起黏土层的塑性变形(图6c, 图6e, 图6f, 图9), 部分黏

土层则因有机质进入层间导致两个黏土层排布呈一定角度(图9)。可膨胀黏土矿物的单层层间可赋存有机分子^[2, 15, 59], 利用TEM-EDS点分析发现低成熟度的延长组泥页岩中, 复合体中蒙脱石层的能谱图有明显的碳峰(图10a—c), 放大后可看到蒙脱石层的波动以及单层厚度的变化(0.9~2.1 nm), 这表明有机分子可进

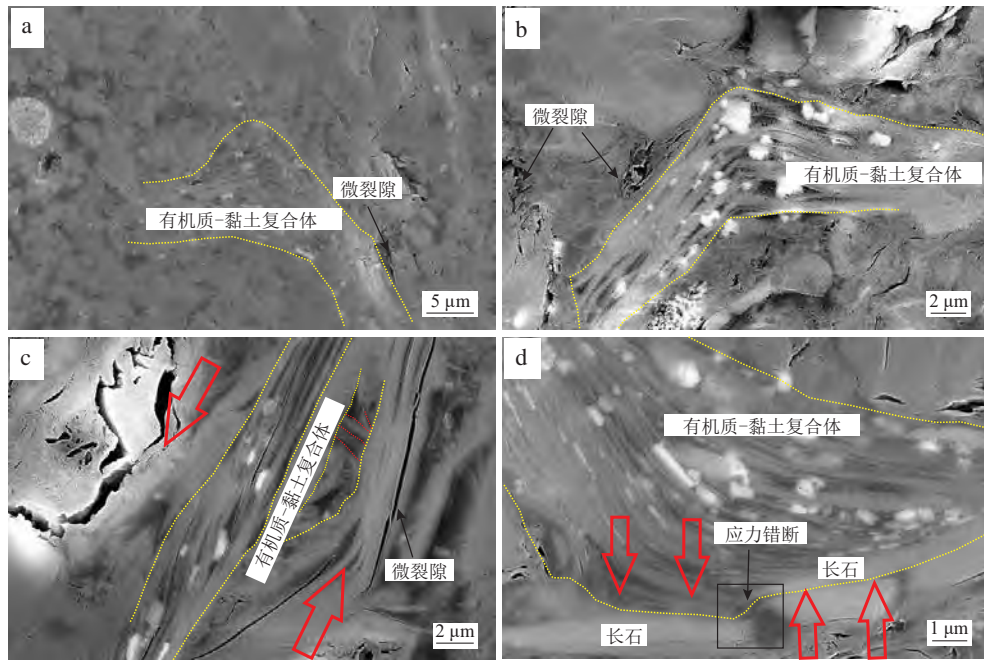


图7 黔北龙马溪组和黔中牛蹄塘组泥页岩中应力作用引起的有机质-黏土复合体变形的SEM图像

Fig. 7 SEM images showing the deformation of organic-clay composites caused by stress in the shale samples from the Longmaxi Formation in northern Guizhou and Niutitang Formation in central Guizhou

a. 龙一段第②层浅钻,深度0.5 m;b. 龙一段第⑤层浅钻,深度0.5 m;c,d. 牛蹄塘组,ZK105钻孔,埋深701.0 m

(红色箭头指示应力方向;黄色和红色虚线指示复合体的延伸方向。)

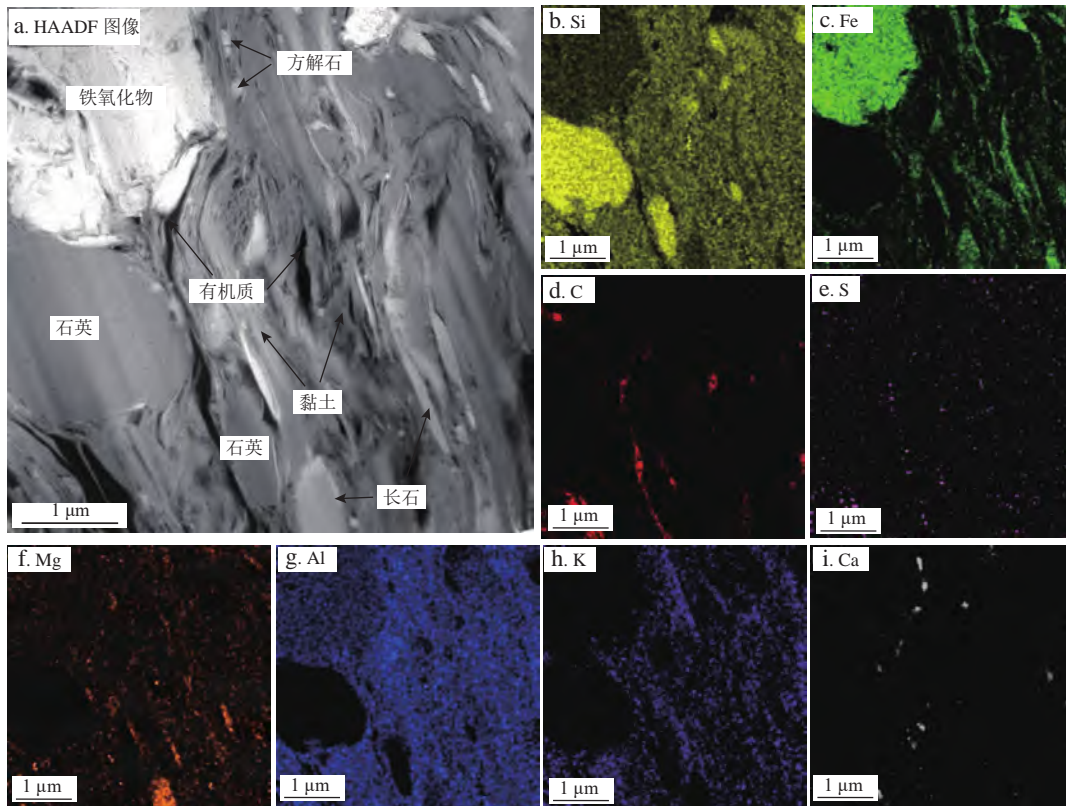


图8 鄂尔多斯盆地长7段941#采油井(深度716 m)泥页岩中有机质-黏土复合体的元素面分布TEM图像

Fig. 8 TEM images showing the element mapping of the organic-clay composites in the shale samples from the Chang 7 Member in producing well 941# (at a depth of 716 m), Ordos Basin

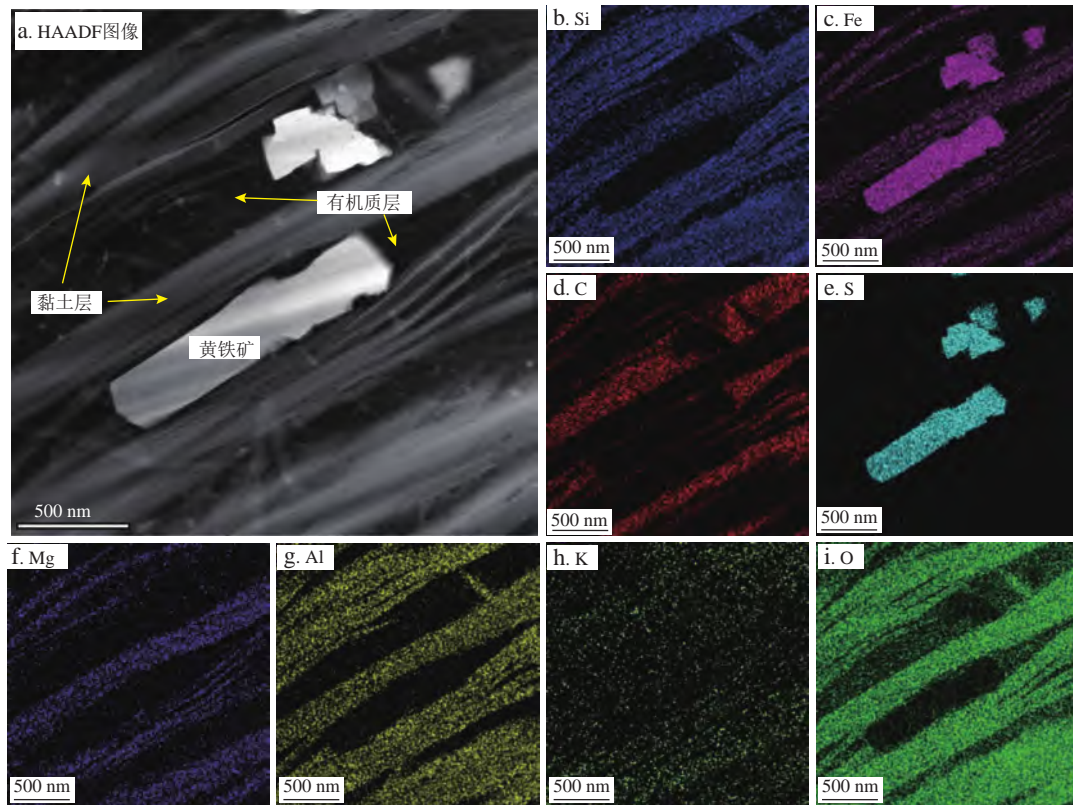


图9 黔北龙马溪组泥页岩龙一段第②层(深度0.5 m)有机质-黏土复合体的元素面分布TEM图像

Fig. 9 TEM images showing the element mapping of the organic-clay composites in the shale samples from layer ② (at a burial depth of 0.5 m) of the first member of the Longmaxi Formation in northern Guizhou

入蒙脱石层间并导致蒙脱石层发生微弱变形。

4.4 黏土矿物转化

泥页岩在成岩演化过程中不仅发生生烃作用,而且还伴随着黏土矿物转化^[60-61]。蒙脱石的伊利石化是热演化过程中最常见的矿物转化,随着热成熟度的增加,伊/蒙混层矿物表现出有序化趋势,即伊/蒙混层中出现更多的伊利石^[15, 24-25]。龙马溪组泥页岩的有机质-黏土复合体中伊/蒙混层发育显著,这种混层矿物的交界处存在明显的黏土层波动(图10d—f),单层厚度变大(最大可达2.2 nm),也引起了一定程度的变形。而牛蹄塘组(图10g, h)和山西组(图10i)泥页岩中的有机质-黏土复合体主要发育伊利石层和绿泥石层(单层厚度较为稳定,分别为1.0 nm和1.5 nm),并未发现伊/蒙混层或绿/蒙混层,推测由于其热成熟度较高而导致黏土矿物转化较为完全,形成了比较稳定的黏土层。

5 有机质-黏土复合体的源-储意义

通过SEM分析,发现赋存于复合体中黏土多层次

间的有机质发育较多纳米孔隙(图3b,图3e,图7b,图7d),这在龙马溪组和牛蹄塘组泥页岩中十分常见。而延长组和山西组泥页岩的复合体中孔隙发育相对较少,可能与其有机质类型有关^[51]。有机质孔隙在复合体中的普遍发育表明这类有机质经历了生烃过程。前人通过对提取的有机质-黏土复合体进行热解-色谱分析发现,通过加热复合体可产生与原油相似的有机组分,也证实了复合体作为生烃母质的巨大潜力^[9]。另外,热演化过程中黏土矿物与有机质之间可发生电子和质子迁移,通过对水分子的吸附和离解,黏土矿物可为有机质的裂解提供氢离子。例如,当黏土矿物表面的吸附水发生脱失时,B酸位可向L酸位转化,进而催化有机质发生热解生烃反应^[62]。值得注意的是,复合体中的黏土矿物和有机质接触面积大,在热演化过程中的物理化学反应充分,既有利于提高黏土矿物的催化活性,也能够促进有机质生烃^[25, 27]。由此可见,除干酪根外,有机质-黏土复合体是泥页岩成岩演化过程中的另一重要烃类来源。

页岩油气储层发育多种类型孔隙,如有机质孔、粒间孔、粒内孔、溶蚀孔等,其中,有机质孔和黏土矿物孔(包括粒间孔、粒内孔等)是烃类储集的重要空间^[63-64]。

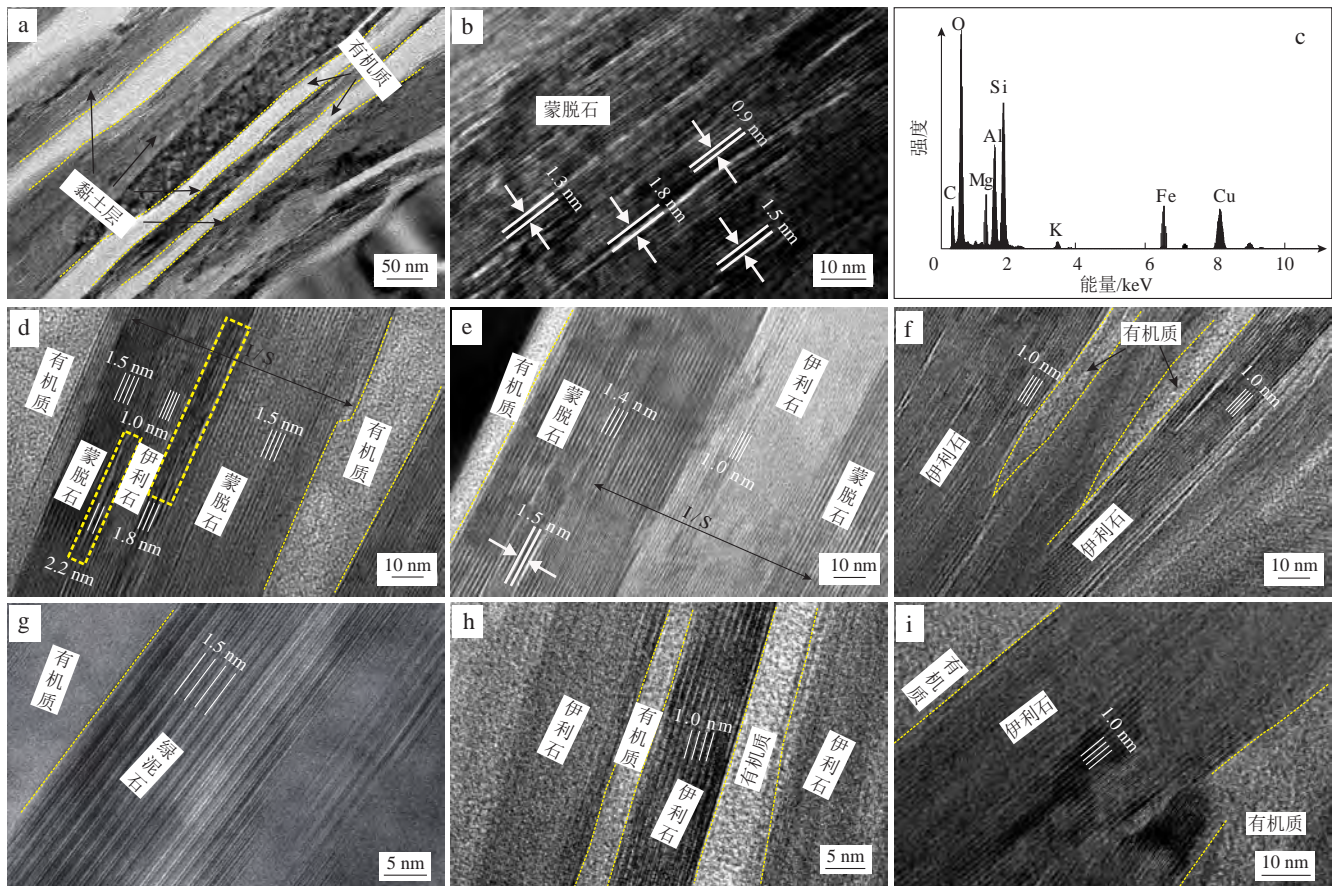


图10 鄂尔多斯盆地延长组、黔北龙马溪组、黔中牛蹄塘组及南华北盆地山西组泥页岩有机质-黏土复合体中有机质的赋存
Fig. 10 Occurrence of organic matter in the organic-clay composites in the shale samples from the Yanchang Formation in the Ordos Basin, Wufeng-Longmaxi formations in northern Guizhou, Niutitang Formation of central Guizhou, and Shanxi Formation in the Southern North China Basin

a—c. 长7段, 941#采油井, 埋深716.0 m, 其中a图显示了黏土多层层间有机质, b图显示黏土单层厚度的变化, c图为a图中“十字”标记处的能谱图, 显示有明显的“碳”峰; d—f. 龙一段第②层浅钻, 深度0.5 m, 显示了明显的伊/蒙混层和不规则的伊利石层; g, h. 牛蹄塘组, ZK105钻孔, 埋深701.0 m, 显示了有机质与绿泥石、伊利石的互层; i. 山西组, ZK02109钻孔, 埋深222.7 m, 显示了有机质与伊利石的互层
(黄色虚线指示黏土层的延伸方向, 白色直线指示黏土层的单层厚度; 除c图外均为TEM图像。)

有机质-黏土复合体是天然的生烃母质, 其中发育的纳米孔隙也可作为烃类的储集空间, 与颗粒有机质和黏土矿物中发育的孔隙相比, 复合体中的孔隙具有一定的特殊性。

首先, 有机质-黏土复合体中的孔隙发育情况受裂隙影响较小。裂隙(构造裂隙或成岩裂隙)可有效提高有机质内部孔隙网络的连通性, 为烃类逸散提供通道^[65]。大量相关研究表明, 四川盆地周缘的牛蹄塘组泥页岩储层中的有机质孔隙十分不发育, 这与微裂隙较为发育(由过高的热演化程度及复杂的地质构造背景引起)密切相关。由图11a—d可见微裂隙对颗粒有机质孔隙发育的重要影响: 由于有机质边缘微裂隙发育, 有机质孔隙网络因相互连通导致烃类散失, 从而降低了有机质孔隙的内部压力, 并在压实作用下导致颗

粒有机质(图11a, c)往往不发育孔隙; 周围无微裂隙发育的颗粒有机质(图11c, d)则发育有较多孔隙。然而, 有机质-黏土复合体周缘存在的微裂隙基本不影响复合体内部的孔隙发育特征(图11e, f): 一方面, 黏土层可降低复合体中的孔隙连通性, 使孔隙难以与外部连通, 减少烃类散失, 孔隙内部压力可抵抗外部压实作用; 另一方面, 两个黏土层之间的狭窄空间(数纳米至上百纳米)可形成强有力的表面张力, 促使多层间有机质稳定吸附于黏土层, 不会因热演化而发生收缩^[66-67]。

其次, 不同应力条件下有机质-黏土复合体中的孔隙发育特征差异较大(图12)。压应力作用下, 复合体几乎不发育孔隙(图12g—i), 当受到变形作用时, 处于拉张环境的有机质往往发育大量孔隙。造成拉张环

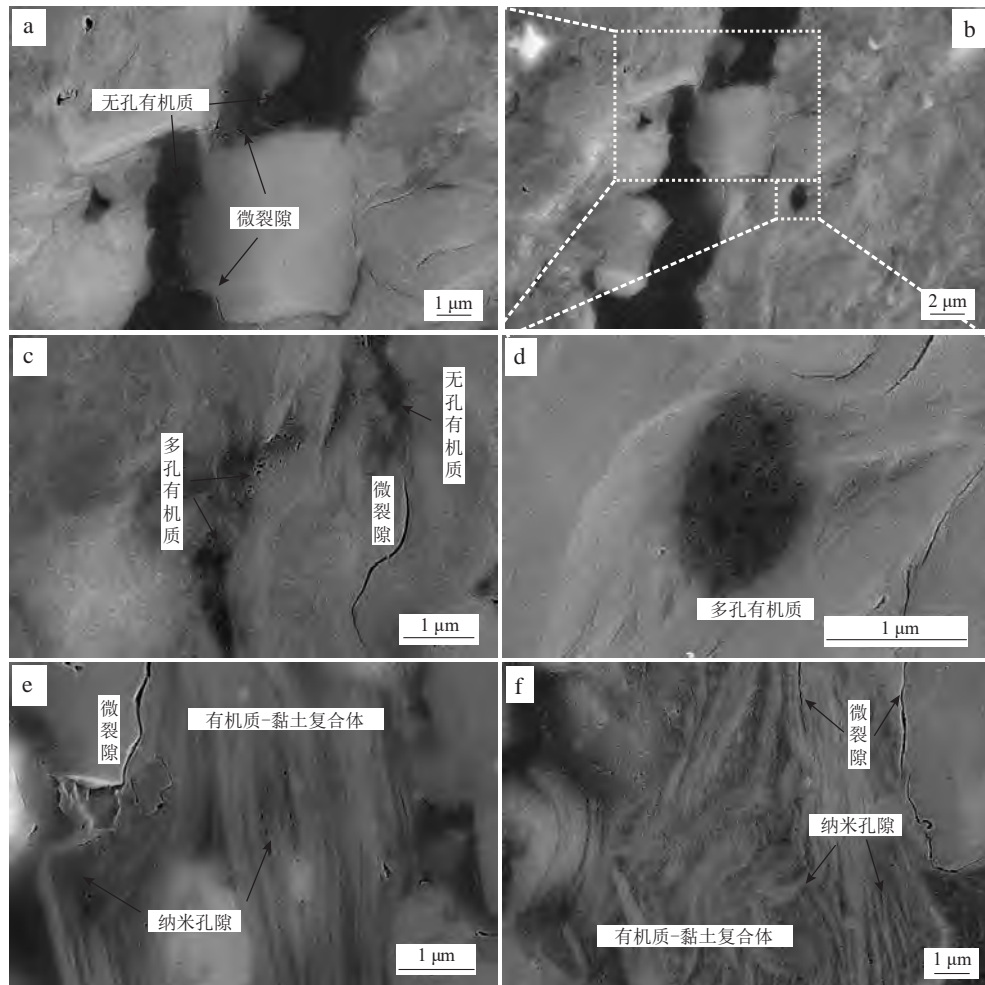


图 11 黔中牛蹄塘组 ZK105 钻孔(深度 701 m)泥页岩中颗粒有机质与有机质-黏土复合体中孔隙发育差异性的 SEM 图像

Fig. 11 SEM images showing the differences of pore development in organic particles and organic-clay composites in the shale samples from the Niutitang Formation in well ZK 105 (at a burial depth of 701 m)

a—d. 表明微裂隙对颗粒有机质中孔隙发育的影响,若颗粒有机质与微裂隙连通,则孔隙不发育,反之,孔隙较为发育;e,f. 显示复合体中的孔隙发育情况不受微裂隙影响

境的原因主要有两个:①复合体中的黄铁矿颗粒能够使黏土矿物两个片层之间形成拉张环境,从而有利于孔隙的发育(图 12a—e)。黄铁矿颗粒的大小决定了拉张环境的强弱:黄铁矿粒径越大,孔隙平均孔径越大,反之越小(图 12c)。②剪切作用也可造成拉张环境,根据黏土矿物的变形方式,可判断剪切应力方向,从而确定黏土层中有机质所处应力环境。如图 12h 和图 12i 所示,因剪应力作用导致复合体发生了明显变形,并在局部形成了拉张环境(图 12h 复合体的核部,图 12i 右侧的复合体),处于拉张环境的有机质形成了大量的纳米孔隙。

综上所述,泥页岩中的有机质-黏土复合体既是重要的生烃母质,也可作为烃类原地储集的重要载体。由构造应力和矿物颗粒作用引起的变形能够改变复合体局部的应力环境,拉张环境可使复合体发育大量的

纳米孔隙,有效提升储集能力。另外,复合体中发育的孔隙因黏土层的保护,不易发生烃类散失,说明复合体发育的孔隙可能储集了一定量的烃类,有利于增加储层的油气资源量。

6 结论

1) 泥页岩中有机质-黏土复合体分布广泛并呈现多种形态特征。根据黏土矿物片层之间的接触方式,可将复合体分为条带状和卡房状;根据复合体是否发生变形,可将其分为原始复合体和变形复合体。多数复合体组成、结构复杂,且发生了不同程度的变形。

2) 有机质-黏土复合体发生变形的机制主要包括以下 4 个方面:复合体外部构造应力引起的变形;复合体内部矿物颗粒(石英、方解石、黄铁矿等)对周围黏土

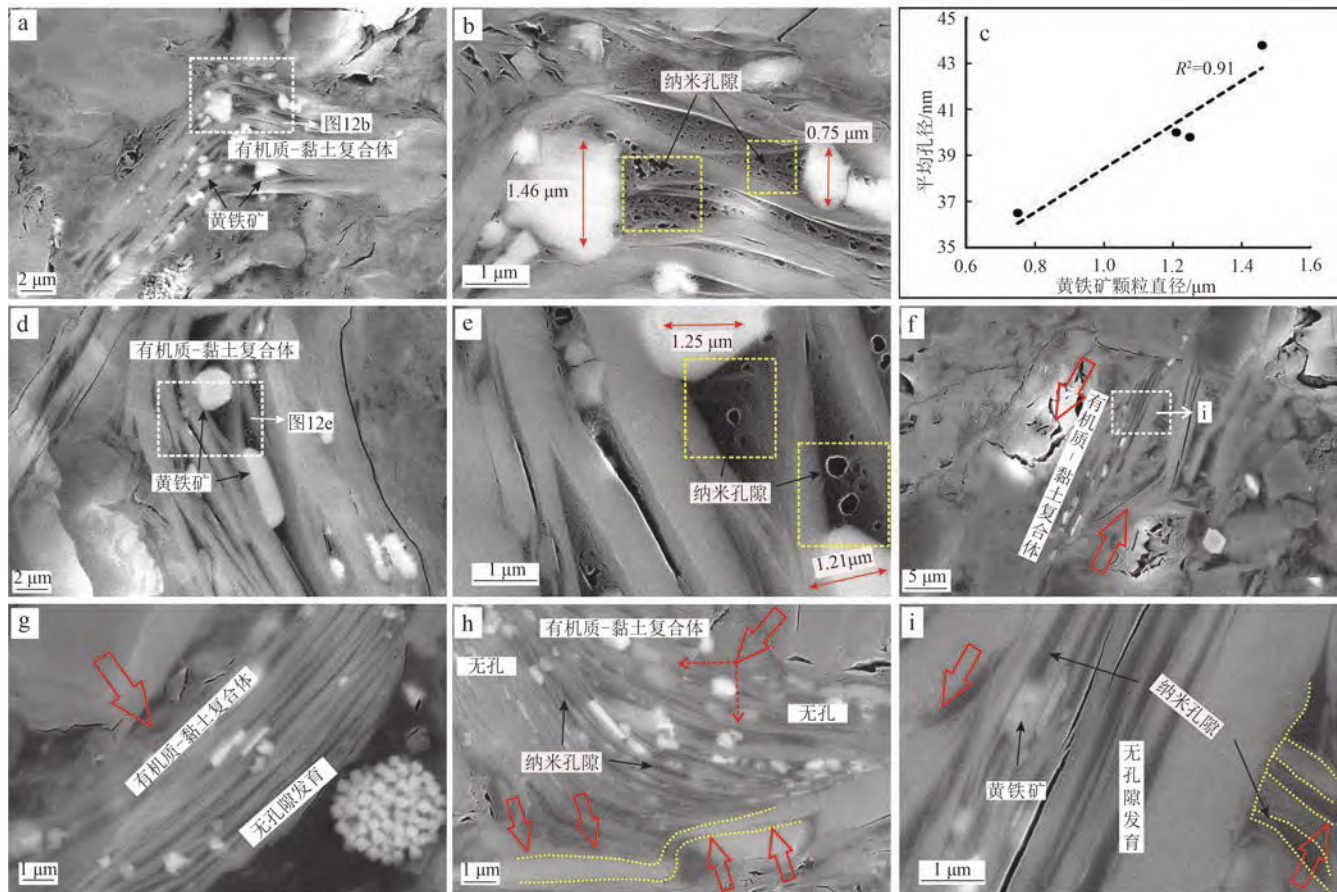


图12 黔北龙马溪组和黔中牛蹄塘组泥页岩在不同应力作用下有机质-黏土复合物中的孔隙发育特征

Fig. 12 The pore development characteristics of organic-clay composites under different stress for the shale samples from the Longmaxi Formation in northern Guizhou, and Niutitang Formation in central Guizhou

a, b. 龙一段第⑤层浅钻, 深度0.5 m; c. 为图b和图e中黄色虚线方框内所有孔隙的平均孔径与对应黄铁矿粒径的相关性图, 表明黄铁矿颗粒对有机质层有支撑作用; d, e. 龙一段第⑧层浅钻, 深度0.6 m; f-i. 牛蹄塘组, ZK105钻孔, 埋深701.0 m, 显示了压应力和剪切应力下的孔隙发育情况 (红色箭头指示应力方向; 黄色虚线指示矿物在应力作用下的延伸方向; 除c图外均为SEM图像。)

层和有机质层的挤压作用; 有机质在黏土矿物单层层间和多层层间的赋存; 黏土矿物转化过程中发生的黏土层波动 (如蒙脱石伊利石化过程引起的单层厚度变化)。

3) 泥页岩中的有机质-黏土复合物既是重要的生烃母质, 也可作为烃类原地储集的重要载体。复合物中局部拉张应力环境可使其发育大量的纳米孔隙, 这类孔隙因黏土层的保护, 不易发生烃类散失, 可有效提升储层的储集能力。

致谢: 感谢论文审稿专家和编辑提出的宝贵建议。

参 考 文 献

[1] CAI Jingong, DU Jiazong, CHAO Qian, et al. Evolution of surface acidity during smectite illitization: Implication for organic carbon cycle [J]. *Marine and Petroleum Geology*, 2022, 138: 105537.

[2] KENNEDY M J, LÖHR S C, FRASER S A, et al. Direct evidence

for organic carbon preservation as clay-organic nanocomposites in a Devonian black shale; from deposition to diagenesis [J]. *Earth and Planetary Science Letters*, 2014, 388: 59-70.

[3] KENNEDY M J, PEVEAR D R, HILL R J. Mineral surface control of organic carbon in black shale [J]. *Science*, 2002, 295 (5555): 657-660.

[4] 蔡进功. 泥质沉积物和泥岩中的有机粘土复合物 [D]. 上海: 同济大学, 2003.

CAI Jingong. Organo-clay complexes in muddy sediments and mudstones [D]. Shanghai: Tongji University, 2003.

[5] 王行信, 万玉兰. 有机粘土复合物在石油生成中的意义 [J]. *中国海上油气*, 1993, 7(2): 27-33.

WANG Xingxin, WAN Yulan. Significance of the organic clay polymer on oil and gas generation [J]. *China Offshore Oil & Gas*, 1993, 7(2): 27-33.

[6] THENG B K G. Formation and properties of clay-polymer complexes [M]. Amsterdam: Soil Elsevier Scientific Publishing Company, 1979: 1-76.

[7] THENG B K G, CHURCHMAN G J, NEWMAN R H. The

- occurrence of interlayer clay-organic complexes in two New Zealand soils[J]. *Soil Science*, 1986, 142(5): 262-266.
- [8] YARIV S, CROSS H. *Organo-clay complexes and interactions* [M]. New York: Marcel Dekker, 2002: 39-112.
- [9] GU Yuantao, LI Xiaoxia, YANG Shuguang, et al. Microstructure evolution of organic matter and clay minerals in shales with increasing thermal maturity [J]. *Acta Geologica Sinica (English Edition)*, 2020, 94(2): 280-289.
- [10] 卢龙飞, 蔡进功, 刘文汇, 等. 泥岩与沉积物中粘土矿物吸附有机质的三种赋存状态及其热稳定性[J]. *石油与天然气地质*, 2013, 34(1): 16-26.
- LU Longfei, CAI Jingong, LIU Wenhui, et al. Occurrence and thermostability of absorbed organic matter on clay minerals in mudstones and muddy sediments[J]. *Oil & Gas Geology*, 2013, 34(1): 16-26.
- [11] CAI Jingong, BAO Yujin, YANG Shouye, et al. Research on preservation and enrichment mechanisms of organic matter in muddy sediment and mudstone [J]. *Science in China Series D: Earth Sciences*, 2007, 50(5): 765-775.
- [12] KENNEDY M J, WAGNER T. Clay mineral continental amplifier for marine carbon sequestration in a greenhouse ocean [J]. *Proceedings of the National Academy of Sciences of the United States of America*, 2011, 108(24): 9776-9781.
- [13] LÖHR S C, KENNEDY M J. Organomineral nanocomposite carbon burial during Oceanic Anoxic Event 2[J]. *Biogeosciences*, 2014, 11(18): 4971-4983.
- [14] BERGAMASCHI B A, TSAMAKIS E, KEIL R G, et al. The effect of grain size and surface area on organic matter, lignin and carbohydrate concentration, and molecular compositions in Peru Margin sediments[J]. *Geochimica et Cosmochimica Acta*, 1997, 61(6): 1247-1260.
- [15] BERTHONNEAU J, GRAUBY O, ABUHAICAL M, et al. Evolution of organo-clay composites with respect to thermal maturity in type II organic-rich source rocks[J]. *Geochimica et Cosmochimica Acta*, 2016, 195: 68-83.
- [16] KEIL R G, HEDGES J I. Sorption of organic matter to mineral surfaces and the preservation of organic matter in coastal marine sediments[J]. *Chemical Geology*, 1993, 107(3/4): 385-388.
- [17] ZHU Xiaojun, CAI Jingong, WANG Guoli, et al. Role of organo-clay composites in hydrocarbon generation of shale [J]. *International Journal of Coal Geology*, 2018, 192: 83-90.
- [18] 刘洪林, 郭伟, 刘德勋, 等. 海相页岩成岩过程中的自生脆化作用[J]. *天然气工业*, 2018, 38(5): 17-25.
- LIU Honglin, GUO Wei, LIU Dexun, et al. Authigenic embrittlement of marine shale in the process of diagenesis [J]. *Natural Gas Industry*, 2018, 38(5): 17-25.
- [19] 聂海宽, 何治亮, 刘光祥, 等. 中国页岩气勘探发现状与优选方向[J]. *中国矿业大学学报*, 2020, 49(1): 13-35.
- NIE Haikuan, HE Zhiliang, LIU Guangxiang, et al. Status and direction of shale gas exploration and development in China [J]. *Journal of China University of Mining & Technology*, 2020, 49(1): 13-35.
- [20] 张鹏辉, 陈志勇, 薛路, 等. 塔里木盆地西北缘下寒武统黑色岩系差异性成岩演化及其影响因素[J]. *岩石学报*, 2020, 36(11): 3463-3476.
- ZHANG Penghui, CHEN Zhiyong, XUE Lu, et al. The differential diagenetic evolution and its influencing factors of Lower Cambrian black rock series in the northwestern margin of Tarim Basin [J]. *Acta Petrologica Sinica*, 2020, 36(11): 3463-3476.
- [21] MASTALERZ M, SCHIMMELMANN A, DROBNIK A, et al. Porosity of Devonian and Mississippian New Albany Shale across a maturation gradient: Insights from organic petrology, gas adsorption, and mercury intrusion[J]. *AAPG Bulletin*, 2013, 97(10): 1621-1643.
- [22] MILLIKEN K L, ESCH W L, REED R M, et al. Grain assemblages and strong diagenetic overprinting in siliceous mudrocks, Barnett Shale (Mississippian), Fort Worth Basin, Texas [J]. *AAPG Bulletin*, 2012, 96(8): 1553-1578.
- [23] WANG Guochang. Deformation of organic matter and its effect on pores in mud rocks [J]. *AAPG Bulletin*, 2020, 104(1): 21-36.
- [24] 李颖莉, 蔡进功. 泥质烃源岩中蒙脱石伊利石化对页岩气赋存的影响[J]. *石油实验地质*, 2014, 36(3): 352-358.
- LI Yingli, CAI Jingong. Effect of smectite illitization on shale gas occurrence in argillaceous source rocks [J]. *Petroleum Geology and Experiment*, 2014, 36(3): 352-358.
- [25] 王行信, 蔡进功, 包于进. 粘土矿物对有机质生烃的催化作用[J]. *海相油气地质*, 2006, 11(3): 27-38.
- WANG Xingxin, CAI Jingong, BAO Yujin. Catalysis of clay mineral to organic matter in hydrocarbon genesis [J]. *Marine Origin Petroleum Geology*, 2006, 11(3): 27-38.
- [26] GU Yuantao, LI Xiaoxia, WAN Quan, et al. The differential evolution of nanopores in discrete OM and organic-clay composites for shale: Insights from stress manipulation [J]. *Arabian Journal of Geosciences*, 2021, 14(7): 554.
- [27] RAHMAN H M, KENNEDY M, LÖHR S, et al. The influence of shale depositional fabric on the kinetics of hydrocarbon generation through control of mineral surface contact area on clay catalysis [J]. *Geochimica et Cosmochimica Acta*, 2018, 220: 429-448.
- [28] 王香增, 张金川, 曹金舟, 等. 陆相页岩气资源评价初探: 以延长直罗一下寺湾区中生界长7段为例[J]. *地学前缘*, 2012, 19(2): 192-197.
- WANG Xiangzeng, ZHANG Jinchuan, CAO Jinzhou, et al. A preliminary discussion on evaluation of continental shale gas resources: A case study of Chang 7 of Mesozoic Yanchang Formation in Zhiluo-Xiasiwan area of Yanchang [J]. *Earth Science Frontiers*, 2012, 19(2): 192-197.
- [29] 张亚雄. 鄂尔多斯盆地中部地区三叠系延长组7段暗色泥岩烃源岩特征[J]. *石油与天然气地质*, 2021, 42(5): 1089-1097.
- ZHANG Yaxiong. Source rock characterization: The dark mudstone in Chang 7 Member of Triassic, central Ordos Basin [J]. *Oil & Gas Geology*, 2021, 42(5): 1089-1097.
- [30] LIU Quanyou, LI Peng, JIN Zhijun, et al. Organic-rich formation and hydrocarbon enrichment of lacustrine shale strata: A case

- study of Chang 7 Member [J]. *Science China Earth Sciences*, 2022, 65(1): 118-138.
- [31] 付金华, 李士祥, 徐黎明, 等. 鄂尔多斯盆地三叠系延长组长7段古沉积环境恢复及意义[J]. *石油勘探与开发*, 2018, 45(6): 936-946.
- FU Jinhua, LI Shixiang, XU Liming, et al. Paleo-sedimentary environmental restoration and its significance of Chang 7 Member of Triassic Yanchang Formation in Ordos Basin, NW China [J]. *Petroleum Exploration and Development*, 2018, 45(6): 936-946.
- [32] 范柏江, 晋月, 师良, 等. 鄂尔多斯盆地中部三叠系延长组7段湖相页岩油勘探潜力[J]. *石油与天然气地质*, 2021, 42(5): 1078-1088.
- FAN Bojiang, JIN Yue, SHI Liang, et al. Shale oil exploration potential in central Ordos Basin: A case study of Chang 7 lacustrine shale [J]. *Oil & Gas Geology*, 2021, 42(5): 1078-1088.
- [33] 杨华, 牛小兵, 徐黎明, 等. 鄂尔多斯盆地三叠系长7段页岩油勘探潜力[J]. *石油勘探与开发*, 2016, 43(4): 511-520.
- YANG Hua, NIU Xiaobing, XU Liming, et al. Exploration potential of shale oil in Chang7 Member, Upper Triassic Yanchang Formation, Ordos Basin, NW China [J]. *Petroleum Exploration and Development*, 2016, 43(4): 511-520.
- [34] 曹尚, 李树同, 党海龙, 等. 鄂尔多斯盆地东南部长7段页岩孔隙特征及其控制因素[J]. *新疆石油地质*, 2022, 43(1): 11-17.
- CAO Shang, LI Shutong, DANG Hailong, et al. Pore characteristics and controlling factors of Chang 7 shale in southeastern Ordos basin [J]. *Xinjiang Petroleum Geology*, 2022, 43(1): 11-17.
- [35] 刘树根, 邓宾, 钟勇, 等. 四川盆地及周缘下古生界页岩气深埋藏-强改造独特地质作用[J]. *地学前缘*, 2016, 23(1): 11-28.
- LIU Shugen, DENG Bin, ZHONG Yong, et al. Unique geological features of burial and superimposition of the Lower Paleozoic shale gas across the Sichuan Basin and its periphery [J]. *Earth Science Frontiers*, 2016, 23(1): 11-28.
- [36] 熊亮. 四川盆地及周缘下寒武统富有机质页岩孔隙发育特征[J]. *天然气地球科学*, 2019, 30(9): 1319-1331.
- XIONG Liang. The characteristics of pore development of the Lower Cambrian organic-rich shale in Sichuan Basin and its periphery [J]. *Natural Gas Geoscience*, 2019, 30(9): 1319-1331.
- [37] 张春明, 张维生, 郭英海. 川东南-黔北地区龙马溪组沉积环境及对烃源岩的影响[J]. *地学前缘*, 2012, 19(1): 136-145.
- ZHANG Chunming, ZHANG Weisheng, GUO Yinghai. Sedimentary environment and its effect on hydrocarbon source rocks of Longmaxi Formation in southeast Sichuan and northern Guizhou [J]. *Earth Science Frontiers*, 2012, 19(1): 136-145.
- [38] 赵建华, 金之钧, 金振奎, 等. 四川盆地五峰组-一龙马溪组页岩岩相类型与沉积环境[J]. *石油学报*, 2016, 37(5): 572-586.
- ZHAO Jianhua, JIN Zhijun, JIN Zhenkui, et al. Lithofacies types and sedimentary environment of shale in Wufeng-Longmaxi Formation, Sichuan Basin [J]. *Acta Petrolei Sinica*, 2016, 37(5): 572-586.
- [39] 王濡岳, 胡宗全, 龙胜祥, 等. 四川盆地上奥陶统五峰组-下志留统龙马溪组页岩储层特征与演化机制[J]. *石油与天然气地质*, 2022, 43(2): 353-364.
- WANG Ruyue, HU Zongquan, LONG Shengxiang, et al. Reservoir characteristics and evolution mechanisms of the Upper Ordovician Wufeng-Lower Silurian Longmaxi shale, Sichuan Basin [J]. *Oil & Gas Geology*, 2022, 43(2): 353-364.
- [40] 谷阳, 徐晟, 徐佳佳, 等. 黔北地区下志留统龙马溪组页岩储层特征[J]. *断块油气田*, 2021, 28(1): 33-39.
- GU Yang, XU Sheng, XU Jiajia, et al. Shale reservoir characteristics of the Lower Silurian Longmaxi Formation in northern Guizhou [J]. *Fault-Block Oil and Gas Field*, 2021, 28(1): 33-39.
- [41] 胡月, 陈雷, 周昊, 等. 海相页岩纹层特征及其对页岩储层发育的影响——以川南长宁地区龙马溪组为例[J]. *断块油气田*, 2021, 28(2): 145-150.
- HU Yue, CHEN Lei, ZHOU Hao, et al. Lamina characteristics of marine shale and its influence on shale reservoir development: A case study of Longmaxi Formation, Changning area, South Sichuan Basin [J]. *Fault-Block Oil and Gas Field*, 2021, 28(2): 145-150.
- [42] 方栋梁, 孟志勇. 页岩气富集高产主控因素分析——以四川盆地涪陵地区五峰组-一龙马溪组一段页岩为例[J]. *石油实验地质*, 2020, 42(1): 37-41.
- FANG Dongliang, MENG Zhiyong. Main controlling factors of shale gas enrichment and high yield: A case study of Wufeng-Longmaxi formations in Fuling area, Sichuan Basin [J]. *Petroleum Geology and Experiment*, 2020, 42(1): 37-41.
- [43] 刘娜娜. 南川地区龙马溪组优质页岩段微观孔隙结构特征[J]. *石油地质与工程*, 2021, 35(4): 21-25.
- LIU Nana. Micro pore structure characteristics of high quality shale section of Longmaxi formation in Nanchuan area [J]. *Petroleum Geology and Engineering*, 2021, 35(4): 21-25.
- [44] 吕艳南, 张金川, 张鹏, 等. 黔西北下寒武统牛蹄塘组页岩气成藏条件与有利勘探区预测[J]. *海相油气地质*, 2015, 20(2): 37-44.
- LYU Yannan, ZHANG Jinchuan, ZHANG Peng, et al. Gas accumulation conditions of Lower Cambrian Niutitang shale and prediction of potential zones in northwestern Guizhou [J]. *Marine Origin Petroleum Geology*, 2015, 20(2): 37-44.
- [45] 祝庆敏, 卢龙飞, 潘安阳, 等. 湘西地区下寒武统牛蹄塘组页岩沉积环境与有机质富集[J]. *石油实验地质*, 2021, 43(5): 797-809, 854.
- ZHU Qingmin, LU Longfei, PAN Anyang, et al. Sedimentary environment and organic matter enrichment of the Lower Cambrian Niutitang Formation shale, western Hunan Province, China [J]. *Petroleum Geology and Experiment*, 2021, 43(5): 797-809, 854.
- [46] 罗超, 刘树根, 罗志立, 等. 贵州黔东南下寒武统牛蹄塘组黑色页岩孔隙结构特征[J]. *地质科技情报*, 2014, 33(3): 93-105.
- LUO Chao, LIU Shugen, LUO Zhili, et al. Pore structure characteristics of black shale in the Lower Cambrian Niutitang Formation of Nangao section in Danzhai, Guizhou Province [J]. *Geological Science and Technology Information*, 2014, 33(3):

- 93-105.
- [47] 王濡岳, 丁文龙, 龚大建, 等. 黔北地区海相页岩气保存条件——以贵州岑巩区块下寒武统牛蹄塘组为例[J]. 石油与天然气地质, 2016, 37(1): 45-55.
WANG Ruyue, DING Wenlong, GONG Dajian, et al. Gas preservation conditions of marine shale in northern Guizhou area: A case study of the Lower Cambrian Niutitang Formation in the Cen'gong block, Guizhou Province [J]. Oil & Gas Geology, 2016, 37(1): 45-55.
- [48] 李中明, 张栋, 张古彬, 等. 豫西地区海陆过渡相含气页岩层系优选方法及有利区预测[J]. 地质前缘, 2016, 23(2): 39-47.
LI Zhongming, ZHANG Dong, ZHANG Gubin, et al. The transitional facies shale gas formation selection and favorable area prediction in the western Henan [J]. Earth Science Frontiers, 2016, 23(2): 39-47.
- [49] 邱庆伦, 张古彬, 冯辉, 等. 河南中牟区块页岩气特征及勘探前景分析[J]. 地质找矿论丛, 2018, 33(1): 70-75.
QIU Qinglun, ZHANG Gubin, FENG Hui, et al. Characteristics of shale gas and analysis of the prospecting potential in Zhongmu block, Henan Province [J]. Contributions to Geology and Mineral Resources Research, 2018, 33(1): 70-75.
- [50] 冯辉, 邱庆伦, 汪超, 等. 南华北盆地中牟凹陷太原组-山西组页岩气成藏特征——以河南中牟区块ZDY2井为例[J]. 地质找矿论丛, 2019, 34(2): 213-218.
FENG Hui, QIU Qinglun, WANG Chao, et al. The shale gas accumulation characteristics of Taiyuan and Shanxi Formations in Zhongmu sag in basins in South of the North China: In case of ZDY2 well of Zhongmu block, Henan Province [J]. Contributions to Geology and Mineral Resources Research, 2019, 34(2): 213-218.
- [51] 谷渊涛, 李晓霞, 万泉, 等. 泥页岩有机质孔隙差异特征及影响因素分析——以我国典型海相、陆相、过渡相储层为例[J]. 沉积学报, 2021, 39(4): 794-810.
GU Yuantao, LI Xiaoxia, WAN Quan, et al. On the different characteristics of organic pores in shale and their influencing factors: Taking typical marine, continental, and transitional facies reservoirs in China as examples [J]. Acta Sedimentologica Sinica, 2021, 39(4): 794-810.
- [52] GU Yuantao, WAN Quan, QIN Zonghua, et al. Nanoscale pore characteristics and influential factors of Niutitang Formation shale reservoir in Guizhou Province [J]. Journal of Nanoscience and Nanotechnology, 2017, 17(9): 6178-6189.
- [53] 吴伟, 王雨涵, 曹高社, 等. 南华北盆地豫西地区C-P烃源岩地球化学特征[J]. 天然气地球科学, 2015, 26(1): 128-136.
WU Wei, WANG Yuhan, CAO Gaoshe, et al. The geochemical characteristics of the Carboniferous and Permian source rocks in the western Henan, the southern North China Basin [J]. Natural Gas Geoscience, 2015, 26(1): 128-136.
- [54] LAGALY G. Principles of flow of kaolin and bentonite dispersions [J]. Applied Clay Science, 1989, 4(2): 105-123.
- [55] O'BRIEN N R. Fabric of kaolinite and illite floccules [J]. Clays and Clay Minerals, 1971, 19(6): 353-359.
- [56] DAY-STIRRAT R J, LOUCKS R G, MILLIKEN K L, et al. Phyllosilicate orientation demonstrates early timing of compactional stabilization in calcite-cemented concretions in the Barnett Shale (Late Mississippian), Fort Worth Basin, Texas (U. S. A) [J]. Sedimentary Geology, 2008, 208(1/2): 27-35.
- [57] LIU Anqi, TANG Dongjie, SHI Xiaoying, et al. Growth mechanisms and environmental implications of carbonate concretions from the ~ 1.4 Ga Xiamaling Formation, North China [J]. Journal of Palaeogeography, 2019, 8(1): 20.
- [58] ZHU Xiaojun, CAI Jingong, LIU Weixin, et al. Occurrence of stable and mobile organic matter in the clay-sized fraction of shale: Significance for petroleum geology and carbon cycle [J]. International Journal of Coal Geology, 2016, 160/161: 1-10.
- [59] BU Hongling, YUAN P, LIU Hongmei, et al. Effects of complexation between organic matter (OM) and clay mineral on OM pyrolysis [J]. Geochimica et Cosmochimica Acta, 2017, 212: 1-15.
- [60] ABID I, HESSE R. Illitizing fluids as precursors of hydrocarbon migration along transfer and boundary faults of the Jeanne d'Arc Basin offshore Newfoundland, Canada [J]. Marine and Petroleum Geology, 2007, 24(4): 237-245.
- [61] HOWER J, ESLINGER E V, HOWER M E, et al. Mechanism of burial metamorphism of argillaceous sediment: 1. Mineralogical and chemical evidence [J]. GSA Bulletin, 1976, 87(5): 725-737.
- [62] 袁鹏. 纳米结构矿物的特殊结构和表-界面反应性 [J]. 地球科学, 2018, 43(5): 1384-1407.
YUAN Peng. Unique structure and surface-interface reactivity of nanostructured minerals [J]. Earth Science, 2018, 43(5): 1384-1407.
- [63] LOUCKS R G, REED R M, RUPPEL S C, et al. Morphology, genesis, and distribution of nanometer-scale pores in siliceous mudstones of the Mississippian Barnett shale [J]. Journal of Sedimentary Research, 2009, 79(12): 848-861.
- [64] WANG Pengfei, JIANG Zhenxue, CHEN Lei, et al. Pore structure characterization for the Longmaxi and Niutitang shales in the Upper Yangtze Platform, South China: Evidence from focused ion beam-He ion microscopy, nano-computerized tomography and gas adsorption analysis [J]. Marine and Petroleum Geology, 2016, 77: 1323-1337.
- [65] SLATT R M, O'BRIEN N R. Pore types in the Barnett and Woodford gas shales: Contribution to understanding gas storage and migration pathways in fine-grained rocks [J]. AAPG Bulletin, 2011, 95(12): 2017-2030.
- [66] ALCOVER J F, QI Y, AL-MUKHTAR M, et al. Hydromechanical effects: (I) on the Na-smectite microtexture [J]. Clay Minerals, 2000, 35(3): 525-536.
- [67] LI Jing, LI Xiangfang, WU Keliu, et al. Water sorption and distribution characteristics in clay and shale: Effect of surface force [J]. Energy & Fuels, 2016, 30(11): 8863-8874.

(编辑 梁慧)